

## Giant spontaneous Hall effect in zero-moment Mn<sub>2</sub>Ru x Ga

Naganivetha Thiyagarajah, Yong-Chang Lau, Davide Betto, Kiril Borisov, J. M. D. Coey, Plamen Stamenov, and Karsten Rode

Citation: [Applied Physics Letters](#) **106**, 122402 (2015); doi: 10.1063/1.4913687

View online: <http://dx.doi.org/10.1063/1.4913687>

View Table of Contents: <http://scitation.aip.org/content/aip/journal/apl/106/12?ver=pdfcov>

Published by the [AIP Publishing](#)

---

### Articles you may be interested in

[Structural, magnetic, and transport properties of sputtered hexagonal MnNiGa thin films](#)

J. Appl. Phys. **116**, 223906 (2014); 10.1063/1.4903943

[Effect of disorder on the magnetic properties of cubic Mn<sub>2</sub>Ru x Ga compounds: A first-principles study](#)

J. Appl. Phys. **116**, 033903 (2014); 10.1063/1.4890229

[Tailoring magnetism of multifunctional Mn x Ga films with giant perpendicular anisotropy](#)

Appl. Phys. Lett. **102**, 132403 (2013); 10.1063/1.4799344

[Effect of mechanical strain on magnetic properties of flexible exchange biased FeGa/IrMn heterostructures](#)

Appl. Phys. Lett. **102**, 022412 (2013); 10.1063/1.4776661

[Strongly correlated electron behavior in R<sub>2</sub>Ru<sub>3</sub>Ga<sub>9</sub> \(R = Ce and U\)](#)

J. Appl. Phys. **107**, 09E113 (2010); 10.1063/1.3365068

---

The advertisement features a photograph of the Model PS-100 cryogenic probe station, which is a complex piece of scientific equipment with various mechanical components and a probe. The background is a gradient of blue. The text is arranged around the image: the model name and description on the left, the company logo on the right, and a slogan at the bottom right.

**Model PS-100**  
Tabletop Cryogenic  
Probe Station



*An affordable solution for  
a wide range of research*

## Giant spontaneous Hall effect in zero-moment $\text{Mn}_2\text{Ru}_x\text{Ga}$

Naganivetha Thiyagarajah, Yong-Chang Lau, Davide Betto, Kiril Borisov, J. M. D. Coey, Plamen Stamenov, and Karsten Rode<sup>a)</sup>

CRANN, AMBER and School of Physics, Trinity College, Dublin 2, Ireland

(Received 9 January 2015; accepted 11 February 2015; published online 24 March 2015)

Spin-dependent transport properties of  $\text{Mn}_2\text{Ru}_x\text{Ga}$  thin-films are studied as function of the Ru concentration and the substrate-induced strain. The large spontaneous Hall angle of 7.7% twenty times bigger than in other 3d metals is a signature of its half-metallicity. The compensation temperature where the magnetization of the two inequivalent antiferromagnetically coupled Mn sublattices cancel can be tuned by varying  $x$  or the biaxial strain. This zero-moment half metal is free from demagnetizing forces and creates no stray field, effectively removing two obstacles to integrating magnetic elements in densely packed, nanometer-scale memory elements, and millimeter-wave generators. © 2015 AIP Publishing LLC. [<http://dx.doi.org/10.1063/1.4913687>]

Cubic ferromagnetic Heusler compounds are a family of materials that often exhibit higher spin polarization at the Fermi level than binary ferromagnetic 3d alloys.<sup>1</sup> Some of the materials are half metals with a gap in the spin-polarized density of states for one spin band which should make them ideal candidates for spin-valves or magnetic tunnel junctions (MTJs).<sup>2–5</sup> Since the prediction by de Groot *et al.*<sup>6</sup> in 1995 of a half metallic material with two inequivalent magnetic sublattices, whose moments precisely cancel, researchers have striven to fabricate such a material. While electronic structure calculations predicted several candidates,<sup>7–9</sup> most attempts to realize such a material had failed.<sup>8,10,11</sup> Kurt *et al.*<sup>12</sup> reported the growth of thin films of near-cubic  $\text{Mn}_2\text{Ru}_x\text{Ga}$  (MRG), where Mn occupies two inequivalent crystallographic positions: 4a and 4c, as shown in Fig. 1. The alloy has been identified as a zero-moment ferrimagnet with high spin polarization, and high  $T_C$  (600 K), showing evidence of half-metallicity. Here, we report on the temperature, Ru concentration, and substrate-induced strain dependence of the transport properties of MRG, at or near the compensation point. Addition of a Ru atom in the cubic  $\text{Mn}_2\text{Ga}$  structure contributes both extra electronic states (12) and electrons (8). Based on the empirical Slater-Pauling rules, this should result in perfect compensation for  $\text{Mn}_2\text{Ru}_{0.5}\text{Ga}$ . The addition of Ru is however likely to change both the shape and the position of the Mn bands leading to a more complex behavior of the magnetic and spin-dependent transport properties. In addition, the tetragonal distortion ( $c/a$  ratio) also influences the band structure. Here, we show that strain is a useful control parameter for engineering the fully compensated MRG half metallic system.

We have previously measured  $L$ -edge X-ray absorption spectroscopy and X-ray magnetic circular dichroism (XAS/XMCD) on the same set of samples used here to determine the site-specific spin and orbital moments as a function of temperature, Ru concentration  $x$ , and substrate-induced strain.<sup>13</sup> We find that there is a temperature depending both on Ru concentration  $x$  and the degree of tetragonal distortion,

where the overall magnetization is perfectly compensated. Crossing this temperature, the spectral features of the dichroic signal change sign, confirming the change of sign of the majority spin channel. We shall demonstrate that this reversal of the direction of the spin polarization corresponds to a sign change of the spontaneous Hall coefficient. We also found evidence of half-metallicity for  $x$  up to 0.7, above which the Fermi level starts to cross the minority spin channel of the Mn in the 4c position.<sup>13</sup> We confirm that the spontaneous Hall angle (SHA) increases as expected substantially, as we decrease the Ru concentration  $x$  from 1.0 to 0.6.

MRG films of thickness ranging from 4 nm to 70 nm were grown on MgO (001) single-crystal substrates by dc-magnetron sputtering at a 250 °C substrate temperature under a base pressure of  $2 \times 10^{-8}$  Torr in a “Shamrock” sputter deposition system. The films were co-sputtered from a  $\text{Mn}_2\text{Ga}$  and a Ru target. The Ru concentration was controlled by keeping the Ru sputtering power fixed while varying that of  $\text{Mn}_2\text{Ga}$ . The films were capped with a  $\sim 2$  nm  $\text{Al}_2\text{O}_3$  layer to prevent oxidation. The crystal structure and lattice parameters were determined by  $2\theta$ - $\theta$  and reciprocal space map (RSM) scans using a BRUKER D8 diffractometer with Cu  $K_{\alpha 1}$  radiation. In order to determine the Ru concentration  $x$ , we deposited four MRG samples with varying  $\text{Mn}_2\text{Ga}$  target power along with a pure Ru film. The density and thickness of the samples were then measured using X-ray reflectivity. Based on the measured density and lattice parameters of these five control samples, we established a relation between the X-ray density and the Ru concentration  $x$ , against which all the samples were measured. The transport measurements were conducted on unpatterned MRG films in a Quantum Design physical properties measurement system (PPMS) for temperatures from 10 K to 400 K. The maximum applied magnetic field,  $\mu_0 H$ , was 12 T.

The out-of-plane lattice parameter  $c$ , determined from  $2\theta$ - $\theta$  X-ray scans, is between 0.598 nm and 0.618 nm, depending on the Ru concentration and the film thickness. We find that  $c$  increases sharply with reducing film thickness. The in-plane lattice parameter  $a$ , determined from reciprocal space mapping was found to be 0.596 nm for all samples,

<sup>a)</sup> Author to whom correspondence should be addressed. Electronic mail: [rodek@tcd.ie](mailto:rodek@tcd.ie)

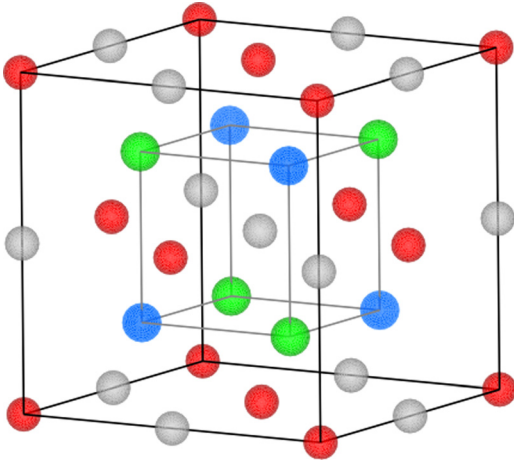


FIG. 1. Crystal structure of  $\text{Mn}_2\text{Ru}_x\text{Ga}$  with Mn in the  $4a$  (red) and  $4c$  (green) sites, Ga in the  $4b$  (grey) site and Ru in the  $4d$  (blue) site.

which precisely matches that of the MgO substrate ( $\sqrt{2}a_0(\text{MgO}) = 0.5956 \text{ nm}$ ). This confirms the cubic character of the MRG films, with a tetragonal distortion ( $(c - a)/a = \Delta c/a$  between 1.8% and 3.6%).

The degree of tetragonal distortion can be controlled by growing MRG thin films on different substrates and/or substrate/seed layer combinations. Another approach to achieve this variation is to grow samples of varying thickness. We recorded RSMs around the symmetric (004) reflection of MRG in order to determine the variation of the lattice

constant  $c$  through the film thickness. The reflections show no clear structure, indicating that the strain is surprisingly homogeneously distributed, and we conclude that the average  $\Delta c/a$  is a good measure of the strain in the samples. The mosaic spread of the MgO substrate is too important to make a quantitative estimate of the variation of the lattice parameter  $c$  through the film thickness. We prepared MRG samples with the same Ru concentration ( $x \sim 1.0$ ) but varying the thickness from 70 nm down to 4 nm, and measured their spontaneous Hall effect (SHE) at different temperatures from 400 K to 10 K in the PPMS. In Fig. 2(a), we show the Hall resistance of one  $\text{Mn}_2\text{RuGa}$  sample ( $x = 1$ ) with  $\Delta c/a = 1.92\%$ , measured between 100 K and 400 K. The sign of the spontaneous Hall coefficient changes between  $T = 300 \text{ K}$  and  $350 \text{ K}$ , consistent with a change of sign of the spin polarization of the carriers at the Fermi level with respect to the net magnetization.

The increase of the out-of-plane lattice parameter  $c$  with reducing sample thickness allows us to control the tetragonal distortion of the samples with similar Ru concentration. From the plot of the temperature derivative of the Hall resistance,  $\partial R_{xy}/\partial T$ , shown in Fig. 2(c), it can be seen that this compensation temperature,  $T_{comp}$ , marked by a peak in the derivative, shifts to lower temperatures as the tetragonal distortion is increased. Perfect compensation is achieved when the two Mn sublattices have equal and opposite magnetizations. This occurs at some particular temperature because the sublattice temperature dependences are different, while the

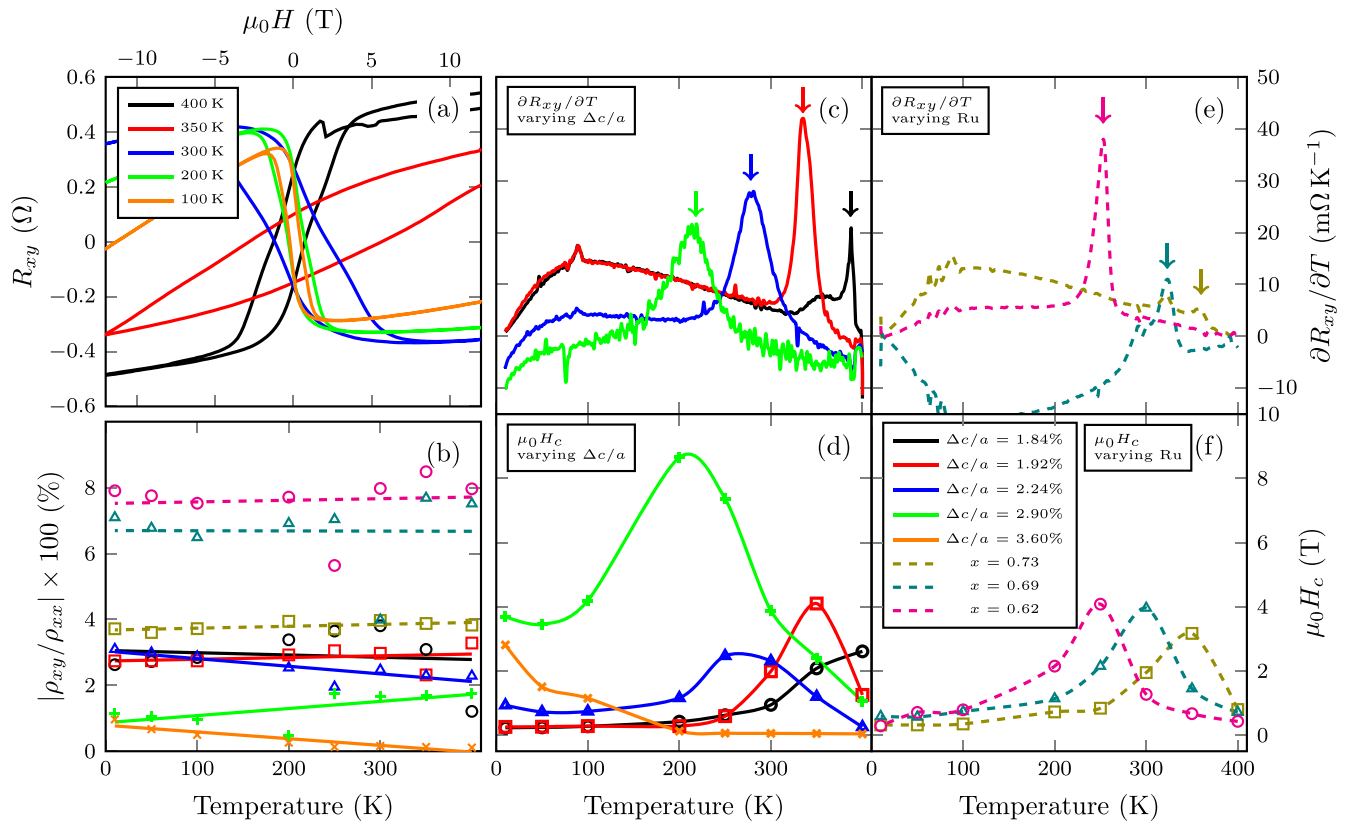


FIG. 2. (a) Spontaneous Hall effect of  $\text{Mn}_2\text{RuGa}$  with  $\Delta c/a = 1.92\%$  at different temperatures. The hysteresis loops have been centered at  $R_{xy} = 0$ . The legend in (f) is common to panels (b)–(f). (b) Magnitude of the SHA as a function of temperature. (c)–(f) Temperature dependent transport properties of two sets of samples; (c) and (d): with the same Ru concentration ( $x \sim 1.0$ ) and varying  $\Delta c/a$  (between 1.8% and 3.6%). (e) and (f): with the same  $\Delta c/a$  ( $\sim 1.9$ ) and varying Ru concentration  $x$  (between 0.62 and 0.73). Panels (c) and (e) show the temperature derivative of the Hall resistance, with a maximum at  $T_{comp}$ , while (d) and (f) trace the temperature evolution of their coercive fields.  $T_{comp}$  is indicated by the arrows in panels (c) and (e).

4a magnetization is practically constant between 2 K and 400 K, the 4c magnetization decreases linearly in the same temperature range.<sup>13</sup> With increasing strain, the zero-temperature magnetization of the 4c Mn sublattice decreases, hence lowering the  $T_{comp}$ . Similarly in the case of varying Ru concentration  $x$ ,  $T_{comp}$  shifts to higher temperatures with increasing  $x$ , as shown in Fig. 2(e). From the SHE measurements, we also note that as the magnetization approaches zero, the coercivity clearly diverges (since the anisotropy field,  $\mu_0 H_a = 2K_{eff}/M_s$ , with  $M_s \sim 0$ ), as shown in Figs. 2(d) and 2(f). As an example, the coercive field of the MRG sample with  $\Delta c/a = 2.90\%$  reaches 9 T at  $T_{comp} \sim 200$  K.

We plot the magnitude of the SHA, defined as  $\rho_{xy}/\rho_{xx}$ , in Fig. 2(b). There are only slight variations in the absolute value with changing temperature. When the SHE loop was measured close to compensation, the films are not fully saturated, and hence, the SHA is somewhat underestimated. In the case of the thinnest sample (4 nm), which also has the largest  $c/a$  ratio, the Curie temperature is shifted to much lower temperatures, as can be inferred from the near-zero SHA, that increases only close to 10 K. This is due to the almost complete loss of magnetic moment carried by the 4c Mn under tetragonal distortion. Extrapolating from our earlier XAS/XMCD measurements, we estimate that the zero-temperature saturation magnetization of this sublattice under a compressive strain of 3.6% is only  $0.25 \mu_B/\text{Mn}$ , compared to  $\sim 1.4 \mu_B/\text{Mn}$  in thicker samples.<sup>13</sup> The much reduced magnetization of this sublattice reduces the magnetic ordering temperature  $T_C$  from  $\sim 550$  K to  $\sim 200$  K, where we first observe appreciable coercivity (see Fig. 2(d)).

Figure 3 shows the evolution of the SHA with varying Ru concentration  $x$  for  $0.6 < x < 1.1$ . From the temperature dependent measurements, we have seen that the SHA is almost constant below  $T_C$ , hence, we compare the SHA at room temperature (300 K). Figure 3 also plots the variation in the room temperature longitudinal resistivity,  $\rho_{xx}$ , and the Hall resistivity,  $\rho_{xy}$ , for the same samples. As can be seen,  $\rho_{xx}$  is predominantly constant over the whole range of  $x$ . The recorded SHA ( $\sim 7.7\%$ ) for samples up to  $x = 0.7$ , which are in the half metallic region, is about an order of magnitude larger than those found for other 3d ferromagnets at room

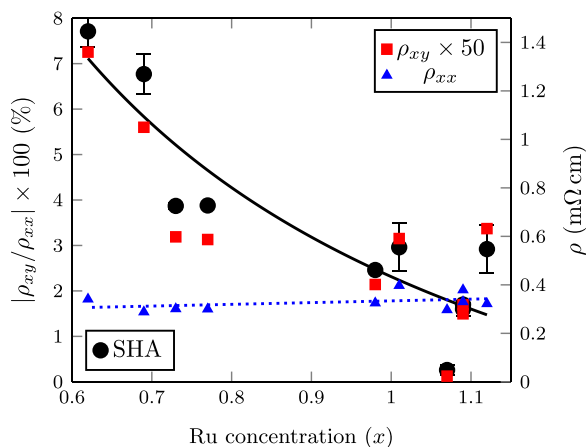


FIG. 3. Evolution of the spontaneous Hall angle,  $\rho_{xy}$  and  $\rho_{xx}$  as a function of Ru concentration  $x$ , extracted from SHE measurements at 300 K. The lines are a guide to the eye.

temperature (0.2%–0.3%),<sup>14</sup> and comparable to values recorded for amorphous rare earth transition metal alloys<sup>15</sup> and dilute magnetic semiconductors such as Mn:GaAs in the degenerate regime.<sup>16</sup> A high SHE is indicative of a low carrier concentration and a high spin polarization. The high SHA was also reported in another Mn-based Heusler alloy,  $DO_{22}$  Mn-Ga,<sup>17</sup> attributed to the high spin polarization of this material.<sup>18</sup> The increase in SHA with decreasing Ru concentration implies that the large SHA is not due to spin-orbit scattering from the addition of Ru, and as it is normalized for effects of changing electronic mobility and carrier concentration, it points to either an extremely high intrinsic contribution to the Hall signal or to an almost complete spin polarization of the carriers close to the Fermi level, as is the case in Mn:GaAs.

In order to examine the effect of the tetragonal distortion on the SHA, we also plot the evolution with  $c/a$  ratio in Fig. 4. As we have seen in Fig. 3, there is a large variation in SHA with the Ru concentration (from 1.0% to 7.7%). Therefore, we have only compared the samples with similar Ru concentrations ( $x \sim 1.0$ ). As the strain increases, the magnetization of the 4c sublattice decreases,<sup>13</sup> resulting in a reduced spontaneous Hall effect. It is unlikely that the effect is directly due to the film thickness, because there is only a weak variation of  $\rho_{xx}$  (see Fig. 4).

We have confirmed that for Ru concentrations in the range of  $\sim 0.6$ – $1.0$ , there is a temperature  $T_{comp}$  where MRG thin films exhibit zero magnetization. The sign of the spontaneous Hall effect reverses at  $T_{comp}$ , indicating inversion of the majority spin channel. The magnitude of the SHA is remarkably large and cannot be attributed to the spin-orbit scattering from Ru, as it increases as  $x$  decreases. It seems to be a signature of the half metallic state. We also show that by varying the tetragonal distortion at a particular Ru concentration, we can tune the compensation of the two Mn sublattices to be in any desired temperature range; at, above or below room temperature.

Recent *ab initio* calculations<sup>19</sup> suggested that a high spontaneous Hall effect and angle could arise from “serious disorder” in MRG samples. This does not explain the clear inversion of the spontaneous Hall loop at  $T_{comp}$ .

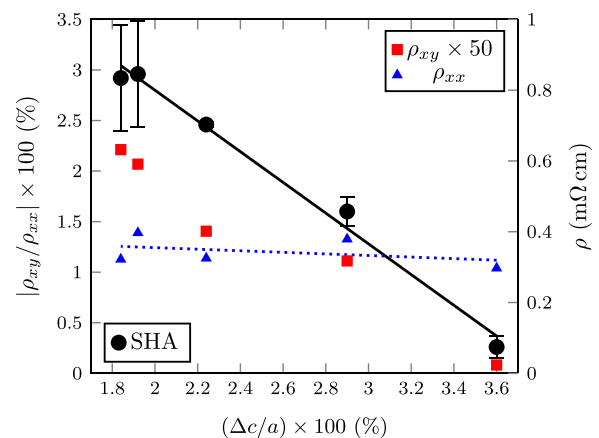


FIG. 4. Evolution of the spontaneous Hall angle,  $\rho_{xy}$  and  $\rho_{xx}$  as a function of the tetragonal distortion ( $c/a$  ratio) extracted from SHE measurements at 300 K for samples with a Ru concentration  $x \sim 1.0$ . The lines are a guide to the eye.



The new class of zero-moment half metallic materials raises several fundamental questions on the nature of magnetism and spin transport in the compensated ferrimagnetic state. The critical current needed to switch the magnetization of the free layer in a Spin Transfer Torque Magnetic Random Access Memory cell (STT-MRAM) is thought to scale with the saturation magnetization  $M_s$ . Even though this scaling is unlikely to apply to ferrimagnets, it is nevertheless expected that for materials like MRG where  $M_s \sim 0$ , switching currents would be reduced, at least on the account of much diminished radiation losses and possibly diminished excitation of low-energy magnons. Furthermore, the ferromagnetic resonance frequency is the upper limit for the switching speed in spin electronic devices such as magnetoresistive memory elements and it determines the output frequency of high-frequency generators based on STT oscillators. The current frontier for information and communication technologies is the “THz gap,” as this spectral range (from 0.1 THz to 10 THz) is not easily accessible.<sup>20</sup> Following Kittel’s equation for magnetic resonance, we have  $\omega_r = \gamma \sqrt{H'_a(2H_{ex} + H'_a)} \approx \gamma \sqrt{2H'_a H_{ex}}$  for an antiferromagnetic sample, where  $H'_a = 2K_u/M_{sl}$  ( $M_{sl}$  the sublattice magnetization) and  $\gamma$  is the gyromagnetic ratio. From the Curie temperature ( $\sim 600$  K) and  $M_{sl}$ , we estimate the exchange field to be  $\mu_0 H_{ex} = 890$  T and the sublattice anisotropy field to be approximately  $\mu_0 H'_a = 0.4$  T. Therefore, the resonance frequency should be of order of 0.75 THz, putting it in the middle of the gap.

In order to utilize MRG in such structures, it is necessary to demonstrate effective spin transport using the new compound, either as polarizer or analyzer in spintronic device structures such as giant or tunnel magnetoresistive stacks, magnetoresistive oscillators, or planar spin Hall effect junctions. We expect that such a demonstration will be achieved in the near future.

This work was supported by Science Foundation Ireland through AMBER, and from the Grant Nos. 13/ERC/I2561

and 11/SIRG/I2130. K.R. acknowledges financial support from the European Community’s Seventh Framework Programme IFOX, NMP3-LA-2010-246102. D.B. acknowledges financial support from IRCSET. The authors would like to thank H. Kurt, M. Žic, and T. Archer for fruitful discussions.

- <sup>1</sup>T. Graf, J. Winterlik, L. MÜchler, G. H. Fecher, C. Felser, and S. S. Parkin, in *Handbook of Magnetic Materials*, edited by K. Buschow (Elsevier, 2013), Vol. 21, pp. 1–75.
- <sup>2</sup>J. Kübler, A. R. William, and C. B. Sommers, *Phys. Rev. B* **28**, 1745 (1983).
- <sup>3</sup>W. Wang, H. Sukegawa, R. Shan, S. Mitani, and K. Inomata, *Appl. Phys. Lett.* **95**, 182502 (2009).
- <sup>4</sup>Y. K. Takahashi, A. Srinivasan, B. Varaprasad, A. Rajanikanth, N. Hase, T. M. Nakatani, S. Kasai, T. Furubayashi, and K. Hono, *Appl. Phys. Lett.* **98**, 152501 (2011).
- <sup>5</sup>S. Tsunegi, Y. Sakuraba, M. Oogane, K. Takanashi, and Y. Ando, *Appl. Phys. Lett.* **93**, 112506 (2008).
- <sup>6</sup>R. A. de Groot, F. M. Mueller, P. G. v. Engen, and K. H. J. Buschow, *Phys. Rev. Lett.* **50**, 2024 (1983).
- <sup>7</sup>S. Wurmehl, H. C. Kandpal, G. H. Fecher, and C. Felser, *J. Phys.: Condens. Matter* **18**, 6171 (2006).
- <sup>8</sup>X. Hu, *Adv. Mater.* **24**, 294 (2012).
- <sup>9</sup>I. Galanakis, P. Mavropoulos, and P. H. Dederichs, *J. Phys. D: Appl. Phys.* **39**, 765 (2006).
- <sup>10</sup>E. Şaşıoğlu, *Phys. Rev. B* **79**, 100406 (2009).
- <sup>11</sup>M. Hakimi, M. Venkatesan, K. Rode, K. Ackland, and J. M. D. Coey, *J. Appl. Phys.* **113**, 17B101 (2013).
- <sup>12</sup>H. Kurt, K. Rode, P. Stamenov, M. Venkatesan, Y.-C. Lau, E. Fonda, and J. M. D. Coey, *Phys. Rev. Lett.* **112**, 027201 (2014).
- <sup>13</sup>D. Betto, N. Thiyagarajah, Y.-C. Lau, C. Piamonteze, M.-A. Arrio, P. Stamenov, J. M. D. Coey, and K. Rode, *Phys. Rev. B* **91**, 094410 (2015).
- <sup>14</sup>J. W. F. Dorleijn, *Philips Res. Rep.* **31**, 287 (1976).
- <sup>15</sup>T. W. Kim, S. H. Lim, and R. J. Gambino, *J. Appl. Phys.* **89**, 7212 (2001).
- <sup>16</sup>Y. Pu, D. Chiba, F. Matsukura, H. Ohno, and J. Shi, *Phys. Rev. Lett.* **101**, 117208 (2008).
- <sup>17</sup>F. Wu, E. P. Sajitha, S. Mizukami, D. Watanabe, T. Miyazaki, H. Naganuma, M. Oogane, and Y. Ando, *Appl. Phys. Lett.* **96**, 042505 (2010).
- <sup>18</sup>H. Kurt, K. Rode, M. Venkatesan, P. Stamenov, and J. M. D. Coey, *Phys. Rev. B* **83**, 020405 (2011).
- <sup>19</sup>I. Galanakis, K. Özdoğan, E. Şaşıoğlu, and S. Blügel, *J. Appl. Phys.* **116**, 033903 (2014).
- <sup>20</sup>J. M. Chamberlain, *Philos. Trans. R. Soc. London, Ser. A* **362**, 199 (2004).